Int. J. Heat Mass Transfer. Vol. 28, No. 5, pp. 1011–1018, 1985
Printed in Great Britain

0017–9310/85 $3.00 + 0.00
Pergamon Press Ltd.

The influence of condensate flow rate on heat transfer in film condensation of stationary vapour on horizontal tube banks

S. S. KUTATELADZE, I. I. GOGONIN and V. I. SOSUNOV

Institute of Thermophysics, Siberian Branch of the USSR Academy of Sciences, Novosibirsk 630090, U.S.S.R.

(*Received* 22 *May* 1984)

Abstract—The paper is a continuation of systematic investigations carried out by the authors in the field of condensation heat transfer. It presents the results of experiments on condensation of practically quiescent vapour on the banks of horizontal smooth tubes of different diameters. The mechanism of heat transfer in condensation of vapour under these conditions has been revealed.

AMONG the factors that determine the intensity of heat transfer in a condenser is a variable condensate flow rate and, as a consequence, the variable hydrodynamics of film flow depending on the location of a tube in a bank. The condensate flow rate, G (kg m^{-1} s^{-1}), is the amount of condensate flowing through a given cross-section over a 1-m wide band. As is shown in ref. [1], the influence of the condensate flow rate in the process of condensation of a practically quiescent vapour is unambiguously determined by the film Reynolds number, at least for the banks of tubes of similar geometries. The results of experiments on heat transfer in film condensation of cooling agents (R21 and R12) in a bank of horizontal tubes for a wide range of condensate flow rate are uniquely correlated in that work by the relation

$$Nu^* = f(Re). \tag{1}$$

The present experiments were conducted on a rig the schematic diagram of which and the experimental procedure are described elsewhere [2]. The schematic diagram of an experimental condenser is presented in Fig. 1. The experiments were carried out with R12 (CF_2Cl_2) condensing on banks composed of 3, 6, 10 and 45 mm dia. tubes. The schematics of the arrangements of tubes in the banks are shown in Fig. 2.

The saturation temperature was determined from the relationship between the pressure and temperature of the substance and was checked by the readings of a thermocouple. The pressure was measured by a manometer of a 0.35 accuracy class. The wall temperature of the test tubes was averaged over the readings of 8 or 10 chromel–coppel thermocouples peened at two sections along the length of the tubes. The heat flux was determined from the cooling water enthalpy. Moreover, measured in the experiments were: the geometric parameters of tubes, spacing of tubes in a bank, the temperature of a condensate at various points between the tubes of a bank. In all the experiments, the vapour velocity at the level of the first upper tube did not exceed 0.05 m s^{-1}, therefore, its effect was not taken into account. The process of condensation was visually observed and recorded by a motion-picture camera through optical windows provided in the experimental condenser. In the course of the experiments, a systematic chromatographic

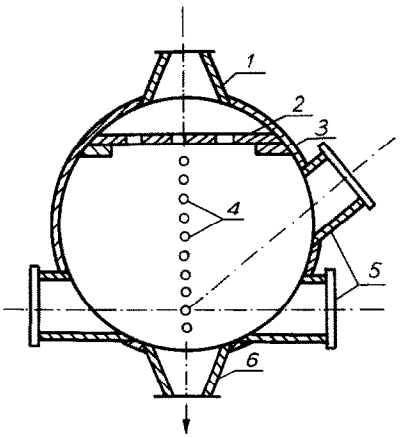

FIG. 1. Schematic diagram of an experimental condenser: (1, 6) inlet and outlet pipes; (2) distribution grid; (3) shell; (4) tube bank; (5) optical windows.

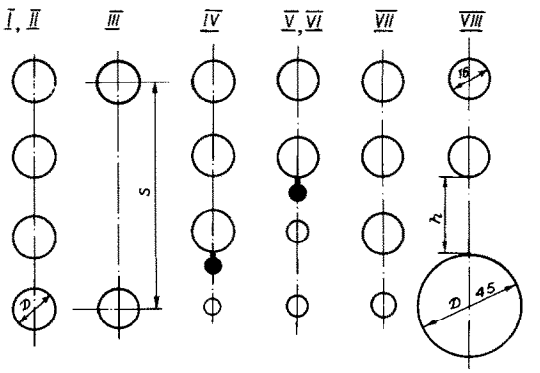

FIG. 2. Schematic diagram of the arrangement of tubes in banks: S, vertical pitch; h, distance between the generators of neighbouring tubes. Uncooled elements are shaded.

NOMENCLATURE

Ar_*	Archimedes criterion based on the capillary constant, $(\sigma^3/v^4\rho^3 g\overline{\Delta\rho})^{1/2}$
c	heat capacity [J kg^{-1} K^{-1}]
D, R	diameter and radius of a tube [m]
$\bar{D}$	dimensionless diameter, $D[g(\rho'-\rho'')/\sigma]^{1/2}$
Ga	Galileo criterion, gL^3/v^2 or $(\pi R)^3 g/v^2$
g	free fall acceleration [m s^{-2}]
L	linear dimension [m]
Nu^*	Nusselt number, $\alpha/\lambda(v^2/g\overline{\Delta\rho})^{1/3}$
Pr	Prandtl number, $c\mu/\lambda$
Re	Reynolds number, $\frac{\pi D}{2}\sum_1^n q_i/\mu r$, where $i = 1,\ldots,n$ is the number of a tube
r	latent heat of evaporation [J kg^{-1}]
q	specific heat flux [W m^{-2}]
$T''', \bar{T}_w$	saturation temperature and mean wall temperature [°C].

Greek symbols

α	heat transfer coefficient [W m^{-2} K^{-1}]
δ	film thickness [m]
λ	thermal conductivity of liquid [W m^{-1} K^{-1}]
μ, v	dynamic and kinematic viscosity of liquid, respectively [Pa s] and [m^2 s^{-1}]
ρ', ρ''	density of liquid and vapour, respectively [kg m^{-3}]
$\overline{\Delta\rho}$	dimensionless complex, $1-\rho''/\rho'$
σ	surface tension [N m^{-1}].

analysis of liquid and vapour phases was made. The air content in the vapour amounted to 0.02–0.03%. The basic conditions of the experiment on the banks are given in Table 1 and Fig. 2. In series V and VI, the seven upper tubes were 16 mm in diameter and only the eighth, ninth, and 10th tubes had the diameters of 6 mm thus providing a sufficiently high condensate flow rate on the ninth and 10th tubes of the bank where the measurements were taken. In series IV, VII and VIII, the banks were assembled from tubes of different diameters, with wetting occurring from the five upper 16-mm diameter tubes. The condensate arrived at the 3- and 6-mm diameter tubes through a supercooled plate and a cylinder (see Fig. 2). The condensate flow rate was varied by changing the temperature of the surrounding water or by cutting off the water supply to the other tubes of the bank.

The influence of free-fall speed on heat transfer was studied on the banks of 16- and 6-mm diameter tubes. In the first case, two tubes above the test one were

Table 1. Conditions for quiescent vapour condensation on tube banks

Series of experiments	Substance	D (mm)	W (m s^{-1})	T'' (°C)	Range of variation ΔT (°C)	Range of variation q (kW m^{-2})	Range of variation W (m s^{-1})	Range of variation Re	Pr	Reference
I	R21	16	0.53	40	2.1–18.2	7.1–34.6	0.53	1.5–420	3.51	[1]
				90	22.0–56	31.5–73			3.46	
II	R12	16	0.53	40	2.3–20.4	4.7–28.7			2.8	
				60	3.7–36.6	6.3–38.2	0.53	3.5–1100	3.43	[1]
				70	38.0–43.7	46–56			3.82	
				80	44.5–54.5	50.0–65.4			4.35	
III	R12	16	1.22	40	2.8–19.4	5.5–28.8	1.22	8–185	2.8	[3]
				60	34.0–36.8	39.8–50.2		70–505	3.43	
IV	R12	3	0.55	40	1.6–13.5	7.1–34		1.0–40	2.8	
				60	27–28	58–61	0.55	35–143	3.43	[4]
				85	42–44	82–86		79–100	4.92	
V	R12	6	0.35	40	2.6–19.3	5.6–33.2	0.35	5–200	2.8	[3]
				60	28.9–31.2	45.6 51.7		57–520	3.43	
VI	R12	6	0.7	40	1.2–25.8	3.9–44.8	0.7	2.3–207	2.8	[3]
				60	30.7–32.0	50.2–57.3		35–535	3.43	
VII	R12	10	0.81	40	16.6–17.6	20.0–22.0	0.81	27–157	2.8	[4]
				60	43.3–38.1	39.6–47.6		93–395	3.43	
VIII	R12	45	0.79	40	2.1–15.6	3.7–16.8		8.0–232	2.8	
				60	28.8–31.5	28.3–35.5	0.79	110–570	3.43	[3]
				85	44.1–50.9	42.7–46.1		608–680	4.92	

removed allowing an increase in the free-fall speed of the liquid by more than a factor of two. The bank of 6-mm diameter cylinders was assembled so that there were two test tubes with spacings $S/D = 2$ and $S/D = 5$. Between the 16-mm diameter tubes, thermocouples were placed to determine the temperature of the condensate at various points. Below the test section, at distances 1, 2, 4, and 6.4 mm from the latter, capillaries of 1.6 mm in diameter and 50 mm long were located horizontally in which thermocouples had been enclosed. Their hot junctions in the middle were rigidly fixed to the capillary walls. The capillaries were placed at different locations along the length of the tube. Thermocouple V (see Fig. 8) was imbedded at the frontal point of the lower uncooled cylinder.

At $Re > 50$, the condensate ran off as stream filaments [Fig. 3(a)]. The spacing between the streamlets, recorded by a high-speed camera, was less than 8 mm at all the temperatures. For this reason, the capillary was always covered with liquid and its temperature, considered to be the mean temperature of the condensate at a given point, was virtually unchanged under the specified conditions. It should be noted that the capillaries with the first and second thermocouples were always covered with liquid which had not been broken off completely from the wall.

Visual observations and high-speed motion pictures have shown that, depending on the heat flux and saturation temperature, there are three distinct types of condensate flow with transitional regimes in between. At small heat fluxes the liquid ran off as separate drops. As the condensate flow rate increased, the breakaway frequency of droplets increased too and ultimately the stream filaments were formed. At small surface tensions ($T'' = 70$ and 85°C) and high condensate flow rates, the condensate ran off as a continuous film [Fig. 3(b)]. The governing parameter of the run-off regime is, presumably, the Ar_* number. The estimates made by the relations suggested in ref. [5] for a film flow from a plate yield the values of the characteristic numbers, $Re_* = f(Ar_*)$, close to those obtained in the present experiments. Here Re_* is based on the condensate flow rate corresponding to the beginning of continuous film formation. The photographs of the condensate flow regimes are given in Fig. 3. Figure 4 presents the photograph of the film surface clearly revealing the places where the streams hit the film on the lower tube. In these places, craters are formed and waves between the streamlets arise. While propagating towards each other, the waves bring about a local thickening of the film halfway between the streamlets. Before the thickened film has a chance to disintegrate, it runs off the surface of the cylinder.

The experimental results on condensation heat

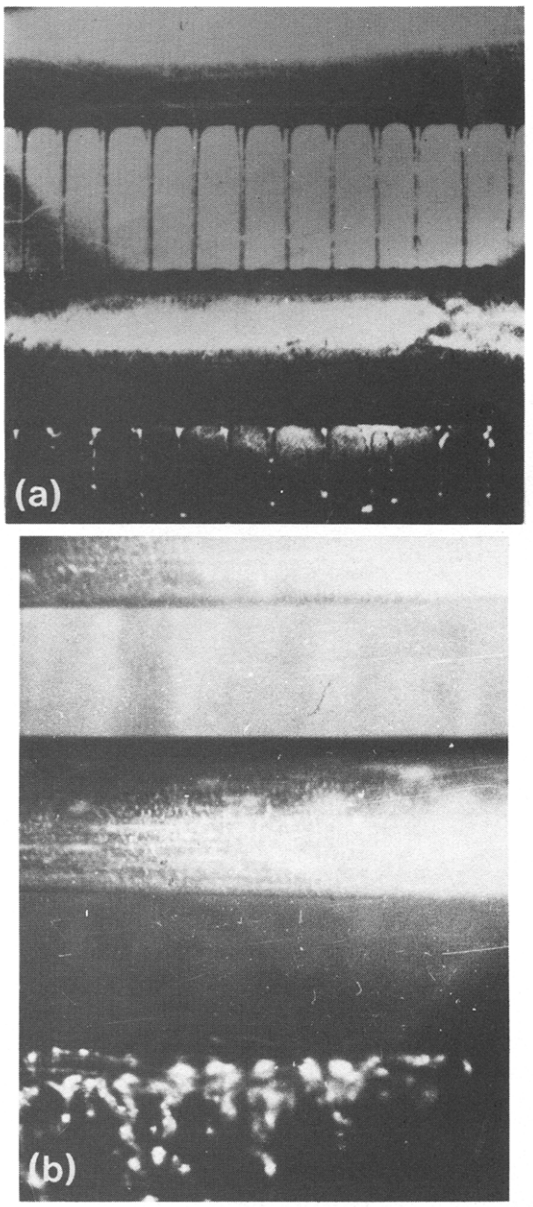

FIG. 3. Characteristic regimes of condensate flow, $D = 16$ mm: (a) stream filaments, $T'' = 60$°C, $Re = 40$; (b) continuous film, $T'' = 85$°C, $Re = 130$.

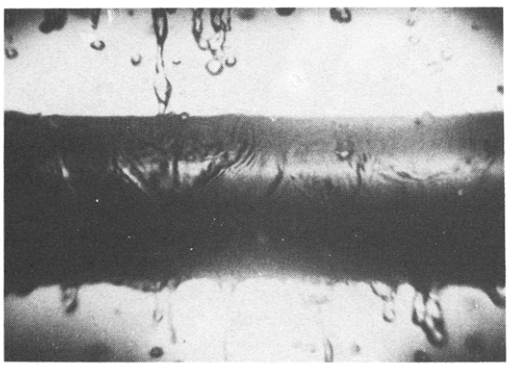

FIG. 4. Condensation of R12 on a tube bank: $D = 16$ mm, $S/D = 1.87$, $T'' = 40$°C, $Re = 130$. Speed: 1100 frames s^{-1}.

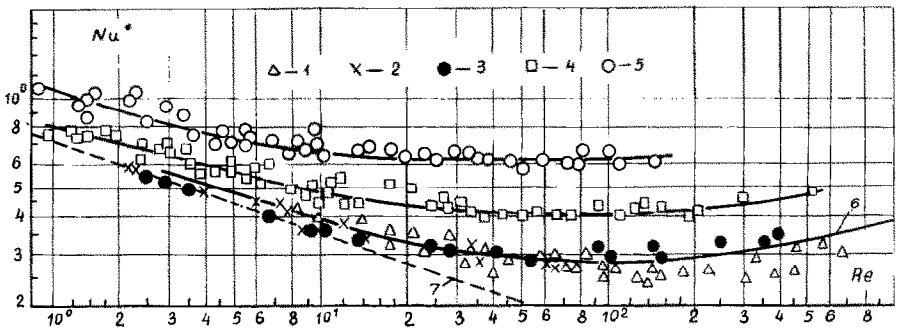

FIG. 5. Heat transfer in condensation of R12 on the banks of tubes of different diameters: (1) $D = 45$; (2) 16; (3) 10; (4) 6.0; (5) 3.0 mm; (6) line averaging the experiments [1]; (7) calculation by the Nusselt theory [6].

transfer on the banks composed of tubes of different diameters are presented in Fig. 5. It is seen that in the case of R12 condensation, the data for the banks of 10-, 16-, and 45-mm diameter tubes are nearly the same and also agree with the experimental results reported in ref. [1]. On the banks of 6- and 3-mm diameter tubes, a pronounced intensification of heat transfer is observed. Common to all the banks is the existence of an extensive region of heat transfer quasi-self-similarity with respect to the Reynolds number. On tubes of smaller diameters the region begins at smaller Reynolds numbers. For the processing of the experimental data obtained at $T'' = 70$–$85°C$ for turbulent film flow regimes ($Re \geqslant Re_{cr}$), a correction factor $(Pr/Pr_0)^{0.4}$ [7] was introduced, being the ratio of the Prandtl number at the temperature of the experiment to the value of Pr_0 at $T'' = 60°C$. Re_{cr} is the critical film Reynolds number for the laminar-wave to turbulent flow transition as defined in ref. [8].

In the quasi-similarity region, the heat transfer intensification on the banks of small diameter tubes is more appreciable than in the case of condensation on single cylinders, as is evident from Fig. 6.

The experimental results on heat transfer in condensation of R12 on single tubes of different diameters agree satisfactorily with the results reported in ref. [1] where it was noted that on cylinders of small diameters at $Re \leqslant 5$ the heat transfer rate increased by about a factor of 1.4 as compared with Nusselt's prediction [6]. In the quasi-self-similarity region, the heat transfer on a 3-mm diameter tube bank is by about a factor of 2.3 higher than for tube banks with $\bar{D} \geqslant 20$.

The experimental results of series II–III and V–VI show (Fig. 7) that an increase in the condensate free-fall speed by more than a factor of 2 results in an insignificant increase of heat transfer. A similar conclusion had been drawn earlier in ref. [9].

A fundamentally important result is given in Fig. 8 which shows characteristic distributions of the temperature T_C in the intertube space. It follows from the figure that the supercooled condensate becomes quickly warmed up and arrives at the lower tube with a temperature close to the saturation one testifying to the occurrence of vapour condensation on streamlets and drops. It is seen that the speed of the warming-up of the liquid grows with the condensate flow rate. The results make it possible to assume that in the quasi-self-similarity region the mechanisms of heat transfer on the banks of tubes of different diameters differ.

In fact, if the temperature of the condensate falling onto the lower tube of the bank is close to the saturation temperature, this means that the condensation has started at a certain distance above the tube. This distance is determined by the point at which the thermal boundary layer (Fig. 9), developing from the wall, emerges onto the film surface. Over the starting length x_i, convective heat transfer occurs. In this case, the following situations can take place [10]:

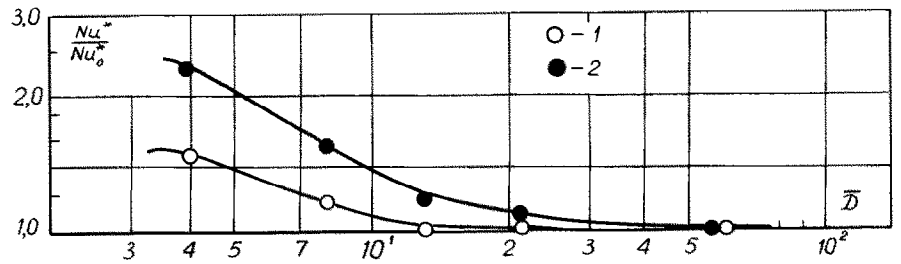

FIG. 6. Dependence of the relative Nusselt number on a dimensionless diameter for condensation on single cylinders (1) and banks (2): (1) $Re = 3.0$; (2) $Re = 150$. Nu_0^*, Nusselt number for $\bar{D} \geqslant 20$.

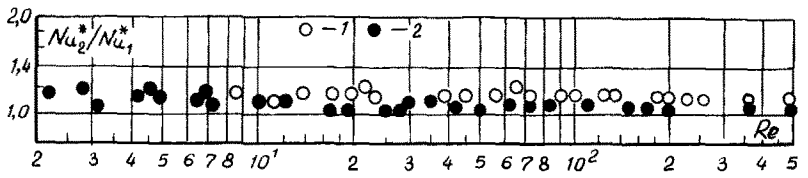

FIG. 7. Influence of the free-fall speed of condensate on heat transfer: (1) $D = 16$ mm; (2) $D = 6.0$ mm. Nu_2^* and Nu_1^*, experimental values of the Nusselt numbers on banks with large and small spacings, h, respectively.

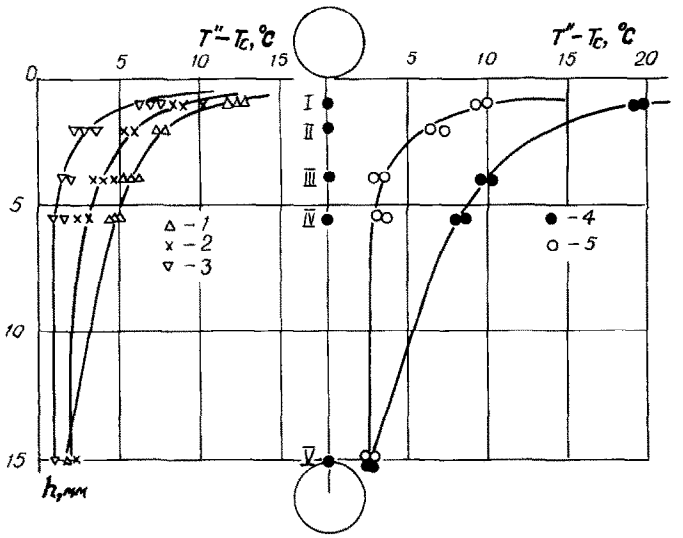

FIG. 8. Temperature profiles of liquid in the intertube space and the diagram of the arrangement of thermocouples: $T'' = 60°C, \Delta T = 35°C$; (1) $Re = 35$; (2) 150; (3) 250. $T'' = 70°C, \Delta T = 50°C$; (4) $Re = 60$; (5) 250. I–V, points of location of thermocouples.

(a) The starting length exceeds the half-perimeter of the tube. The liquid is supercooled due to convection, and condensation occurs entirely in the intertube space on drops and streamlets.

(b) When $x_i \ll \pi R$, condensation on a tube bank occurs practically in the same manner as on a vertical surface. The estimates of condensation heat transfer on a vertical surface, based on the investigations of the hydrodynamics of films and on the measurements of the 'residual' thickness, have been made in ref. [11] by employing the 'residual' thickness of a film being almost insensitive to the Reynolds number, which was discovered in ref. [18] and confirmed repeatedly later [12].

The assumption that the thermal resistance of the film can be substituted by the thermal resistance of the 'residual' thickness allows the following relation to be obtained for the Nusselt number in the quasi-self-similarity region

$$Nu_c^* = 0.527\, Ar_*^{-1/15}. \qquad (2)$$

(c) When the starting length x_i is less than the tube half-perimeter, $L = \pi R$, both convective heat transfer and condensation take place. Over the starting length, a thermal boundary layer develops whose thickness increases and at $x = x_i$ it reaches the thickness of the film. Downstream, over the section $L - x_i$, the condensation of vapour occurs on the surface of the film.

The problem of heat transfer with laminar flow of the film down a flat vertical plate of length L, where a thermal boundary layer develops, was considered in ref.

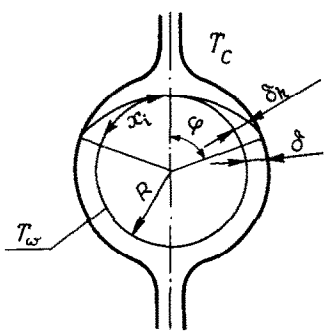

FIG. 9. A simplified diagram of liquid flow in a bank and the scheme of problem formulation [14].

Table 2. Values of $P(\varphi)$, $Q(\varphi)$, $Q(\varphi)/\varphi$

φ (degrees)	$P(\varphi)$	$Q(\varphi)$	$Q(\varphi)/\varphi$
0	0	0	0
10	0.073	0.260	1.49
20	0.184	0.489	1.401
30	0.315	0.697	1.331
40	0.460	0.896	1.283
50	0.615	1.088	1.247
60	0.779	1.272	1.215
70	0.948	1.449	1.186
80	1.120	1.619	1.160
90	1.295	1.783	1.135
100	1.469	1.939	1.111
110	1.641	2.088	1.088
120	1.810	2.229	1.064
130	1.974	2.361	1.040
140	2.129	2.483	1.016
150	2.273	2.594	0.991
160	2.404	2.696	0.965
170	2.515	2.777	0.936
180	2.589	2.884	0.899

[13]. The expression for the mean Nusselt number over the starting length $x_i = L$ is as follows

$$\alpha L/\lambda = 0.91\, Pr^{1/3} Re^{1/9} (L/(\nu^2/g)^{1/3})^{2/3} \quad (3)$$

or

$$Nu_t^* = 0.91\, Pr^{1/3} Re^{1/9} Ga^{-1/9}. \quad (4)$$

The problem of convective heat transfer in a laminar film flow down a $2R$-diameter horizontal tube, over which a thermal boundary layer δ_h develops, was solved in ref. [14]. The angle φ, at which the thermal boundary layer attains the thickness of the film, can be calculated from the expression

$$P(\varphi) = \int_0^{\varphi} (\sin\varphi)^{1/3}\, d\varphi = 0.605\, Pr\, Re^{1/3} Ga^{-1/3} \quad (5)$$

and from Table 2 where the values of the function $P(\varphi)$ are given. The relation suggested in that work to determine the Nusselt number over the starting length can be presented as

$$Nu_t^* = 1.13\, Pr^{1/3} Re^{1/9} Ga^{-1/9} Q(\varphi)/\varphi \quad (6)$$

where

$$Q(\varphi) = \int_0^{\varphi} [(\sin\varphi)/P(\varphi)]^{1/3}\, d\varphi$$

is also given in Table 2. It is important to observe that the expressions for the Nu_t^* number obtained from equations (4) and (6) differ only by the coefficient. Common to the both equations is the dependence of heat transfer on the linear dimension of the heat transfer surface and equally slight dependence on the film Reynolds number.

Table 3. Calculated results of heat transfer in condensation of R12

Re	50	100	150	200	250	300	400
$D = 3$ mm; $T'' = 40°C$; $Re_i = 100$; $Nu_c^* = 0.241$							
$\bar{x}_i$	0.38	1.00					
Nu_c^*	0.43	0.35	0.37	0.38	0.39	0.40	0.41
$\overline{Nu}^*$	0.31	0.35	0.37	0.38	0.39	0.40	0.41
$D = 3$ mm; $T'' = 85°C$; $Re_i = 63.4$; $Nu_c^* = 0.270$							
$\bar{x}_i$	0.69						
Nu_c^*	0.47	0.43	0.45	0.47	0.48	0.49	0.50
$\overline{Nu}^*$	0.41	0.43	0.45	0.47	0.48	0.49	0.50
$D = 6$ mm; $T'' = 60°C$; $Re_i = 143$; $Nu_c^* = 0.249$							
$\bar{x}_i$	0.28	0.60					
Nu_t^*	0.39	0.37	0.32	0.33	0.33	0.34	0.35
$\overline{Nu}^*$	0.29	0.32	0.32	0.33	0.33	0.34	0.35
$D = 10$ mm; $T'' = 60°C$; $Re_i = 210$; $Nu_c^* = 0.249$							
$\bar{x}_i$	0.19	0.39	0.62	0.90			
Nu_t^*	0.34	0.33	0.32	0.29	0.28	0.29	0.30
$\overline{Nu}^*$	0.27	0.28	0.29	0.29	0.28	0.29	0.30
$D = 16$ mm; $T'' = 60°C$; $Re_i = 229$; $Nu_c^* = 0.249$							
$\bar{x}_i$	0.14	0.27	0.42	0.57	0.75	1.0	
Nu_t^*	0.31	0.30	0.30	0.29	0.28	0.25	0.25
$\overline{Nu}^*$	0.25	0.26	0.27	0.27	0.27	0.25	0.25
$D = 45$ mm; $T'' = 40°C$; $Re_i = 763$; $Nu_c^* = 0.241$							
$\bar{x}_i$	0.06	0.10	0.16	0.21	0.27	0.32	0.43
Nu_t^*	0.22	0.22	0.22	0.22	0.22	0.22	0.22
$\overline{Nu}^*$	0.24	0.24	0.24	0.24	0.24	0.23	0.23
$D = 45$ mm; $T'' = 85°C$; $Re_i = 481$; $Nu_c^* = 0.270$							
$\bar{x}_i$	0.08	0.17	0.26	0.34	0.43	0.53	0.74
Nu_t^*	0.026	0.26	0.26	0.26	0.25	0.25	0.24
$\overline{Nu}^*$	0.27	0.27	0.27	0.26	0.26	0.26	0.24

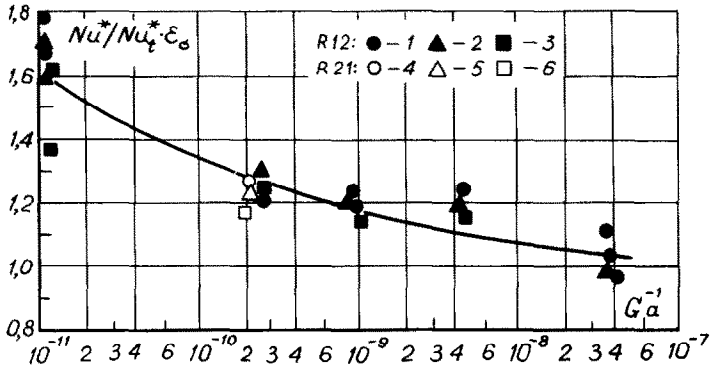

FIG. 10. Comparison between the averaged experimental Nusselt numbers, Nu^*, and those calculated by equation (8) depending on the Galileo criterion: 1.4, $Re = 100$; 2.5, $Re = 150$; 3.6, $Re = 300$.

Table 3 lists the results of the calculations of:
—the ratio of the starting length to the tube half-perimeter, $x_i = x_i/\pi R$, by equation (5);
—Nu_t^* over the starting length, by equation (6);
—Nu_c^* for condensation, by equation (2);
—Re_i at $\varphi = \pi$, by equation (5);
—Nu^* number for mixed heat transfer, by the formula

$$\overline{Nu^*} = (Nu_t^* x_i + Nu_c^*(\pi R - x_i))/\pi R. \quad (7)$$

The calculations have been performed for the conditions under which the experiments were carried out. Depending on the experimental conditions, the starting length at $Re \leqslant Re_i$ ranged from $0.06\pi R$ to πR. In this case, both convective heat transfer and condensation take place.

A simplified schematic diagram of liquid flow on a tube bank in the form of a continuous film, given in Fig. 9, certainly differs from the real one. The calculated starting lengths also seem to somewhat differ from those existing in reality, but nevertheless they testify to the possibility of different means of heat transfer.

At $Re > Re_i$, the starting length exceeds the half-perimeter of the tube and over this length only convective heat transfer occurs, which, at $\varphi = \pi$, is calculated by equation (6) as

$$Nu_t^* = 1.01\, Pr^{1/3} Re^{1/9} Ga^{-1/9}. \quad (8)$$

In Fig. 10, the results of experiments on heat transfer are compared with those calculated by formula (8). It is seen that heat transfer on the banks composed of small-diameter tubes tends to the predicted value. Figure 11 presents a comparison between the results of experiments and those calculated by equation (7) for the condensation of vapour of two liquids on the banks of tubes of different diameters at different saturation temperatures.

The agreement between the experimental and predicted results on heat transfer coefficients may be considered as satisfactory, especially if one takes into account that the suggested calculation scheme has been to a considerable extent simplified as compared with the actual process of heat and mass transfer in banks.

While processing the experimental results presented in Figs. 10 and 11, it was assumed that the influence of the surface tension forces on heat transfer is the same on both single cylinders and the banks composed of these cylinders. The experimental value of the Nu^* number for 3- and 6-mm diameter cylinders has been corrected by employing a correction factor ε_σ which is equal to 1.4 and 1.15 according to ref. [1].

The terms in equation (7) which determine the overall heat transfer have one feature in common, i.e. they both are almost independent of the film Reynolds number. The linear dimension of the cylinder in expression (6), as

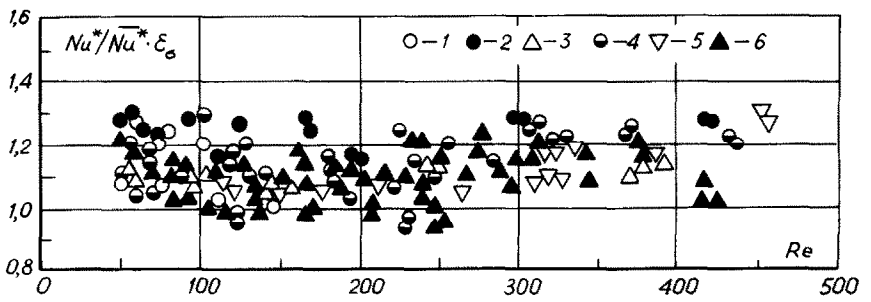

FIG. 11. Comparison of the experimental data with the results calculated from equation (7). R 12: (1) $D = 3$; (2) 6; (3) 10; (4) 16; (5) 45 mm; R 21: (6) $D = 16$ mm.

well as the increasing fraction of the convective term in equation (7) yield a perceptible increase in the overall heat transfer in condensation on small-diameter tube banks.

CONCLUSIONS

As a result of the experimental investigation of heat transfer in condensation of practically quiescent vapour on the banks of horizontal tubes of different diameters, it has been established that:

(1) The heat transfer in the intertube space in the case of vapour condensation on supercooled drops and discrete liquid streamlets contributes substantially to the heat transfer at $Re > 50$. Liquid arrives at a lower tube in a bank at a temperature which is close to the saturation temperature, thus inducing the formation of the thermal boundary layer starting length. In this section, convective heat transfer takes place.

(2) The starting length of the thermal boundary layer depends on both the film Reynolds number and the diameter of the cylinder. The latter circumstance, as well as the influence of the surface tension forces, leads to an appreciable intensification of heat transfer on small-diameter tube banks.

(3) The experimental results agree satisfactorily with the heat transfer calculations by the scheme suggested in this paper.

REFERENCES

1. S. S. Kutateladze and I. I. Gogonin, Heat transfer in film condensation of slowly moving vapour, *Int. J. Heat Mass Transfer* **22,** 1593–1599 (1979).
2. I. I. Gogonin, A. P. Dorokhov and V. I. Sosunov, Heat transfer in film condensation of quiescent vapour. Preprint of the Institute of Thermosphysics, Siberian Branch of the USSR Acad. Sci. No. 44–80, Novosibirsk (1980).
3. I. I. Gogonin, V. I. Sosunov, S. I. Lazarev and O. A. Kabov, Heat transfer in condensation of quiescent vapour on the banks of horizontal tubes of different geometries, *Teploénergetika* **3,** 33–36 (1982).
4. I. I. Gogonin, V. I. Sosunov, S. I. Lazarev and O. A. Kabov, Investigation of heat transfer by condensation of quiescent vapour on the banks of horizontal tubes of different diameters, *Teploénergetika* **3,** 17–19 (1983).
5. R. Puzyrewski and E. E. Zukoski, Disintegration of a liquid sheet due to gravity force, *Fluid Dynam. Trans.* **4,** 619–633 (1969).
6. W. Nusselt, Die Oberflächenkondensation Wasserdampfes, *Z. Ver. dt. Ing.* **60,** 541–546 (1916).
7. S. S. Kutateladze, *Fundamentals of Heat Transfer.* Atomizdat, Moscow (1979).
8. H. Brauer, Strömung und Wärmeübergang bei Reisefilmen, *VDI Forsch Hft.* **457, 1–40** (1956).
9. S. S. Kutateladze, Heat transfer in film condensation on horizontal tubes, *Sov. Kotloturbostr.* **10,** 434–438 (1938).
10. I. I. Gogonin and V. I. Sosunov, Generalization of experimental data on condensation of quiescent vapour on horizontal tube banks, *Teor. Osnovy Khim. Tekhnol.* **18,** 56–62 (1984).
11. S. S. Kutateladze, I. I. Gogonin and N. I. Grigoriyeva, Analysis of heat transfer in film condensation of quiescent vapour on a vertical surface, *J. Engng Phys.* **44,** 885–894 (1983).
12. S. V. Alekseyenko, V. Ye. Nakoryakov and B. G. Pokusayev, Waves on the surface of vertical falling liquid film. Preprint of the Institute of Thermosphysics, Siberian Branch of the USSR Acad. Sci. No. 36-79, Novosibirsk (1979).
13. V. Ye. Nakoryakov and N. I. Grigoriyeva, Calculation of heat and mass transfer in nonisothermal absorption over the starting length of a falling film, *Teor. Osnovy Khim. Tekhnol.* **14,** 483–488 (1980).
14. I. T. Rogers, Laminar falling film and heat transfer characteristics on horizontal tubes, *Can. J. Chem. Engng* **59,** 213–222 (1981).

INFLUENCE DU DEBIT DE CONDENSAT SUR LE TRANSFERT THERMIQUE DANS LA CONDENSATION EN FILM D'UNE VAPEUR STATIONNAIRE SUR DES RANGEES DE TUBES HORIZONTAUX

Résumé—Le texte est la suite de recherches systématiques conduites par les auteurs dans le domaine du transfert thermique en condensation. Il présente les résultats des expériences sur la condensation d'une vapeur pratiquement immobile sur des rangées de tubes lisses et horizontaux de diamètres différents. Le mécanisme du transfert thermique en condensation, dans ces conditions, est élucidé.

EINFLUSS DES KONDENSATSTROMES AUF DEN WÄRMEÜBERGANG BEI DER KONDENSATION VON RUHENDEM DAMPF AN WAAGERECHTEN ROHRBÜNDELN

Zusammenfassung—Diese Arbeit stellt eine Fortsetzung der systematischen Untersuchungen dar, die von den Autoren auf dem Gebiet der Wärmeübertragung bei der Kondensation durchgeführt worden sind. Versuchsergebnisse werden dargestellt, die bei der Kondensation von praktisch ruhendem Dampf an einem Bündel von waagerechten glatten Rohren mit unterschiedlichem Durchmesser gewonnen wurden. Der Wärmeübergangsmechanismus bei der Dampfkondensation unter diesen Bedingungen wird aufgezeigt.

ВЛИЯНИЕ ПЛОТНОСТИ ОРОШЕНИЯ НА ТЕПЛООБМЕН ПРИ ПЛЕНОЧНОЙ КОНДЕНСАЦИИ НЕПОДВИЖНОГО ПАРА НА ПАКЕТАХ ГОРИЗОНТАЛЬНЫХ ТРУБ

Аннотация—Приведены результаты экспериментов по теплообмену при конденсации практически неподвижного пара на пакетах горизонтальных труб разного диаметра. Вскрыт механизм передачи тепла при конденсации пара на пакетах горизонтальных труб.